798 Transaction of the Korean Society of Mechanical Engineers, Vol. 10, No. 5, pp. 798~805, 1986.

<Original>

Natural Convection about a Vertical Flat Plate Immersed in a Thermal Plume

Keun Shik Chang* and Man Yeong Ha**

(Received April 24, 1986)

自由 熱上昇流 中央에 놓인 垂直平板에 관한 自然對流

장 근 식·하 만 영

Key Words; Vertical Plate(垂直平板), Line Heat Source(線熱源), Thermal Interference(熱干涉), Boundary Layer Equations(境界層 方程式), Finite Difference Method(有限差分法)

抄 錄

斷熱 혹은 等溫 境界條件 下의 垂直平板과, 線熱源으로부터 형성되는 熱上昇流 間의 熱的 相互作用을 조사하였다. 境界層 方程式은 Patankar-Spalding의 有限差分法을 사용하여 계산하였다. 斷熱平板의 경우에 自由 熱上昇流로 부터 벽 境界層으로 부터의 점진적인 발달 단계를 설명하였다. 等溫平板의 경우에는 平板주위에 새롭게 형성되는 熱境界層에서의 熱傳達現象을 자세히 考察하였다.

Nomenclature

- g : Gravitational acceleration
- Gr : Grashof number, $g\beta QS^3/k\nu^2$
- k : Thermal conductivity
- Pr : Prandtl number, ν/α
- Q : Heat flux per unit length from the line heat source
- S : Distance between the line heat source and the upper plate
- T : Temperature
- u,v : Streamwise and transverse velocity component, respectively
- U,v : Dimensionless streamwise and transverse velocity component; $U=u/\sqrt{g\beta QS/k}$, $v=v/\sqrt{g\beta QS/k}$
- x,x',y : Streamwise and transverse coordinates, see Fig. 1
- X, Y : Dimensionless coordinates; $X=x/S$, $Y=y/S$
- α : Thermal diffusivity
- β : Thermal expansion coefficient
- δ : Boundary layer thickness
- ν : Kinematic viscosity
- ϕ : Stream function, $\int_0^y u\,dy$
- Ψ : Dimensionless stream function, $\Psi=\phi/\nu$
- θ : Dimensionless temperature, $k(T-T_\infty)/Q$

* Member, Department of Mechanical Engineering Korea Advanced Institute of Science and Technology

** Member, Korea Heavy Industries and Construction Co., Ltd

Subscripts

aw : Adiabatic wall
max : Maximum value at any streamwise station
s : Similarity Solution
w : Wall
∞ : Ambient

Superscripts

′ : Derivative with respect to transverse coordinate
* : Isothermal plate put in a quiescent environment

1. Introduction

An important class of natural convection heat transfer is the one related to the buoyancy driven flows moving freely in an open envirnment. Such flows arise frequently in the nature due to the temperature gradient caused by the natural processes. Under certain circumstances, the interaction of a thermal body with such free boundary layers becomes important in engineering. For example, many thermally active parts in electronic devices are immersed in the thermal plume caused by others. Similar applications could be found in the mechanical systems, nuclear engineering and solar energy collectors.

Zeldovich in Russia in 1937 is the first who described the natural convection plume arising from a horizontal line heat source[1]. In the early 1970's, both Gebhart[1~2] and Fujii[3] found by the similarity method the closed form solution of the boundary layer equation for the plume induced by a horizontal line heat source. In the present paper we treat the thermal interaction of a stationary surface with such a free plume. A semi-infinite flat plate, either adiabatic or isothermal, is situated vertically on the symmetric line of a two-dimensional thermal plume, with the leading edge

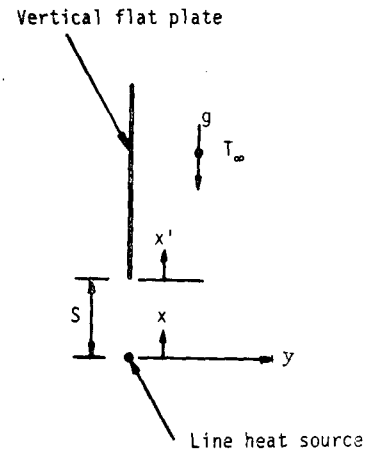

Fig. 1 Schematic diagram of the system

of the flat plate at some distance from the horizontal line heat source; see Fig. 1. The plume, which arrives at the flat plate in a preheated state with a finite velocity, is then significantly affected by the presence of the flat plate. Conversely, the heat transfer characteristics of the flat plate is dependent upon the condition of the impinging plume very much.

Flow regime of the incident plume flow at the leading edge of the plate is determined by the Grashof number based on the distance S and the strength of the line heat source Q. The onset of the transition to turbulence is known to occur at $Gr=6.94\times10^{8}$[3]. In the present study, we restricted our attention to the Grashof number range in which the flow along the plate remains laminar.

2. Governing Equations

We assume that the flat plate is very thin. The mass, momentum and energy boundary layer equations take the form dimensionlessly

$$\frac{\partial U}{\partial X}+\frac{\partial V}{\partial Y}=0 \tag{1}$$

$$U\frac{\partial U}{\partial X}+V\frac{\partial U}{\partial Y}=\theta+Gr^{-0.5}\frac{\partial^2 U}{\partial Y^2} \tag{2}$$

$$U\frac{\partial\theta}{\partial X}+V\frac{\partial\theta}{\partial Y}=Gr^{-0.5}Pr^{-1}\frac{\partial^2\theta}{\partial Y^2} \quad (3)$$

The plume region $(0\leq X<1)$ has the following boundary conditions

$$\frac{\partial U}{\partial Y}=\frac{\partial\theta}{\partial Y}=0 \quad \text{on} \quad Y=0$$
$$U=\theta=0 \quad \text{as} \quad Y\to\infty \quad (4)$$

The wall conditions of the flat plate$(X\geq 1)$ are

$$U=0,\begin{cases}\dfrac{\partial\theta}{\partial Y}=0 \text{ (Adiabatic wall)}\\ \theta=\theta_w \text{ (Isothermal wall)}\end{cases} \quad \text{on } Y=0$$
$$U=\theta=0 \quad \text{as } Y\to\infty \quad (5)$$

Here, in the case of isothermal wall a third parameter θ_w enters the problem.

3. Method of Solution

The above equations are solved numerically using the Patankar-Spalding method[4] in which a coordinate transformation is made to normalize the boundary layer thickness. The Patankar-Spalding method operates in (X, ω) coordinate. The transverse coordinate ω is dimensionless stream function defined by $\omega=(\Psi-\Psi_i)/(\Psi_0-\Psi_i)$, in which Ψ_i and Ψ_0 are the values of the stream function at the inner and outer edges of the boundary layer, respectively. In the present problem, $\Psi=0$ but Ψ_0 varies with X as the boundary layer entrains fluid in the course of its development.

The finite difference grid spans the range $0\leq\omega\leq 1$ at all X, so that as the boundary layer thickness varies, the grid automatically follows the variation. The grid layout encompasses the following features:

(i) Grid points are sufficiently deployed in the range $0\leq\omega\leq 1$. Two hundred points are used for the adiabatic and isothermal vertical flat plate, respectively.

(ii) Variable space is used for the grid system in the ω-direction with the highest concentration near the wall or symmetry line[5].

(iii) A highly refined and carefully distributed grid points are used in the X-direction in the wall boundary layer region. Here, the step size DX in the X-direction is to be determined in the numerical computational processes.

The present governing equations are parabolic type; velocity and temperature profiles are required at an initial plane in the stream direction. In the present paper, boundary layer calculation is initiated from an initial plane near the line heat source, where a closed form solution is available. The initial data are taken from the solution of the integral momentum and energy equation.

$$U=0.8Gr^{-0.1}Pr^{-0.4}X^{0.2}F \quad (6)$$
$$\theta=0.3654Gr^{-0.2}Pr^{-0.8}X^{-0.6}F \quad (7)$$

where

$$F=1-6(y/\delta)^2+8(y/\delta)^3-3(y/\delta)^4 \quad (8)$$

These initial profiles where transformed as a function of ω by the bisection method.

As a check on the accuracy of the present finite difference computation, the centerline temperature obtained by the present method is

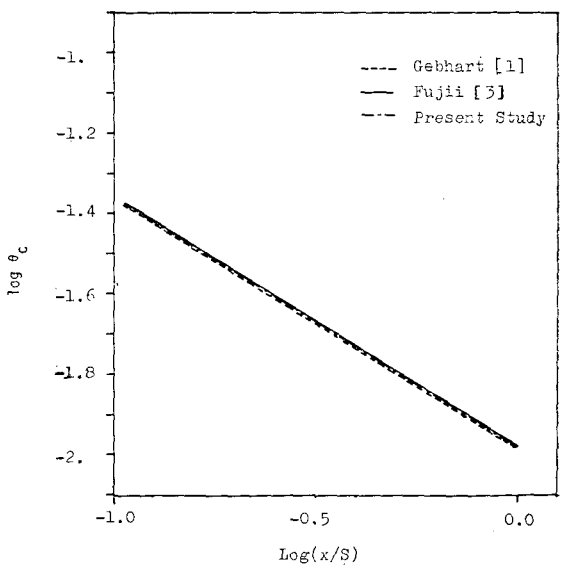

Fig. 2 Comparison of data

compared with that in references (1) and (3) in the plume region. In Fig. 2, the function $\mathrm{Log}\theta_c$ is presented as function of Log (x/S). The close agreement between the different three methods are quite noteworthy. Especially, the present method gave a result that agrees with Fujii *et al.*[8] up to the impressive first four digits below the decimal.

4. Results and Discussion

4.1 Adiabatic Flat Plate

The streamwise variation of the maximum velocity and the maximum temperature can be viewed in Fig. 3 for different Prandtl numbers. It is clearly observable that the viscous drag exerted by the flat plate contributes to lowering the maximum velocity in the initial stage right after the impingement of the plume on the flat plate. This velocity retardation is seen increased in its degree for more viscous or higher Prandtl number fluid in Fig. 3. The initial retardation occurs more rapidly for higher Prandtl number, see the slope near $\log(x/S)=0$. After this initial stage, however, the maximum velocity is increased constantly through the

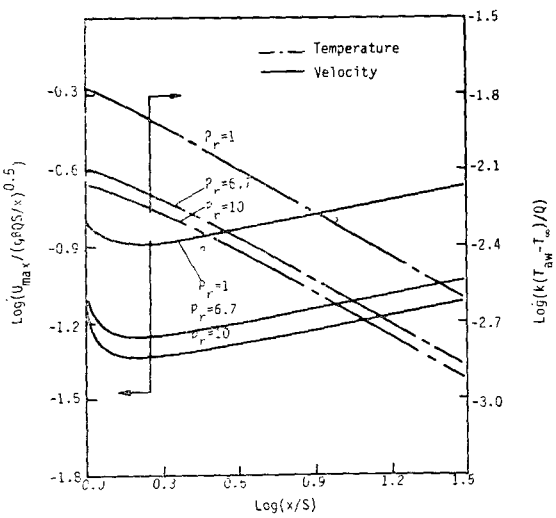

Fig. 3 Adiabatic wall temperature and maximum velocity for the wall plume ($Gr=10^7$).

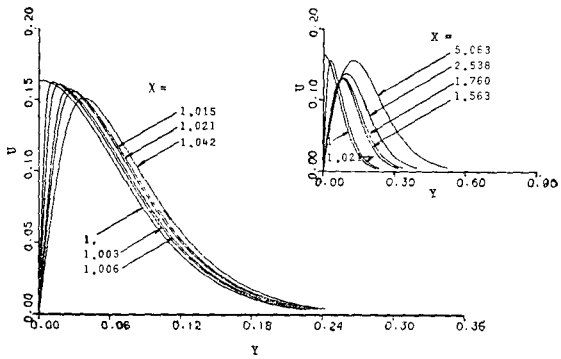

Fig. 4(a) Velocity profiles for the wall boundary layer, $Pr=1$, $Gr=10^7$

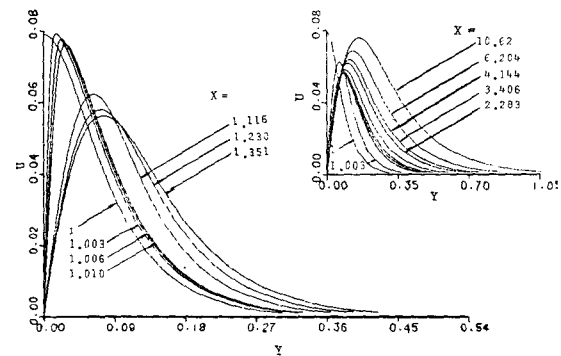

Fig. 4(b) Velocity profiles for the wall boundary layer, $Pr=6.7$, $Gr=10^7$

continued action of buoyancy force, obeying a power law

$$u_{\max}/(g\beta Qs/k)^{0.5}\sim(x/S)^{0.2} \tag{9}$$

Remarkablely, this 0.2 power dependence is identical to that of the similarity solution given in the case when a line heat source is attached to the very tip of the flat plate[7]. Therefore, the x/S value at which the power-law dependence begins to be effective can be regarded as a measure of distance in which the wall plume is developing.

On the other hand, the maximum temperature is decreased continuously in the stream direction to settle down to a power law

$$k(T_{aw}-T_\infty)/Q\sim(x/S)^{-0.6} \tag{10}$$

With increasing Prandtl number, the maximum temperature decreases more slowly in the initial stage before it tends to a regular decrease

governed by the above power-law relation. This (-0.6) power variation also corresponds to the similarity wall plume given in the reference (6).

In the figures 4(a) and 4(b), the aforementioned initial velocity retardation phenomenon can be seen more explicitly. The velocity profiles of the impinging shear flow is rapidly deformed to accomodate the sudden change in the velocity boundary condition from Neumann to Dirichlet type. It is noted that Y-position of the maximum velocity is moved away from the wall as the flow is convected downstream in the boundary layer: see Fig. 5, also.

In contrast, for the isothermal wall shown in Fig. 9, the flow is suddenly faced with the same no-slip condition at the isothermal plate but is more rapidly accelerated in the downstream direction due to the greater buoyancy force than the case of the adiabatic wall. In this case again, the boundary layer rapidly approaches to the similarity profile in the downstream direction.

Another viewpoint on the development of the adiabatic wall boundary layer can be conveniently represented by the velocity profiles in Fig. 5. The scaled velocity $U/U_{\max}$ is shown as a function of $Y/X^{0.4}$ for $Pr=1$ and $Gr=10^7$. When the profiles are fully developed, they fall on a single similarity curve in the downstream direction. For $Pr=1$, it takes about $X\cong 4$ until the similarity is obtained. However, for $Pr=6, 7$ and 10 the velocity profiles are fully developed at about $X\cong 10$: the figure is not shown here. Thus, the distance of the initial flow stage is increased with Prandtl number. It is seen from these figures that there is a significant profile change between the free plume and the fully developed flow.

Similarly, the temperature curves are shown in terms of $k(T-T_\infty)/Q$ versus Y in Figs. 6 (a) and 6(b). In Fig. 7 the normalized temperature $(T-T_\infty)/(T_{aw}-T_\infty)$ is similarly plotted as a function of $(Y/X^{0.4})$ for $Pr=1$ and $Gr=10^7$. In contrast to the velocity, the temperature

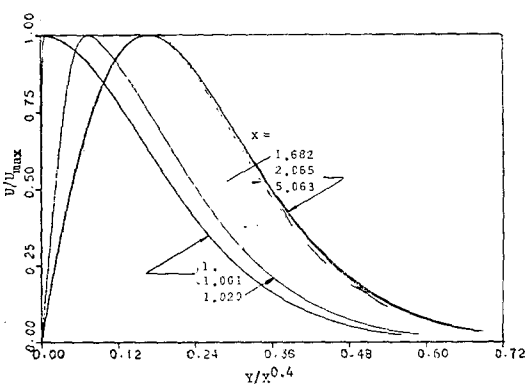

Fig. 5 Locally normalized velocity profiles, $Pr=1$, $Gr=10^7$

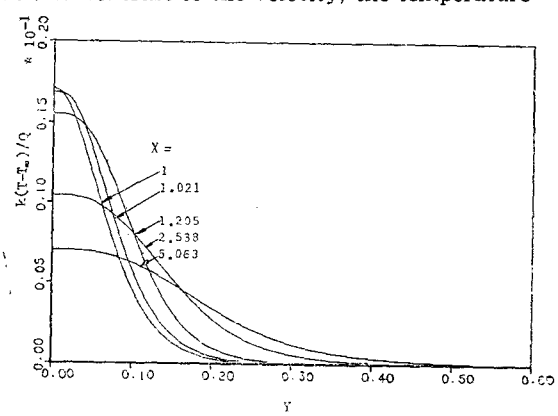

Fig. 6(a) Tempreature profiles for the wall boundary layer, $Pr=1$, $Gr=10^7$

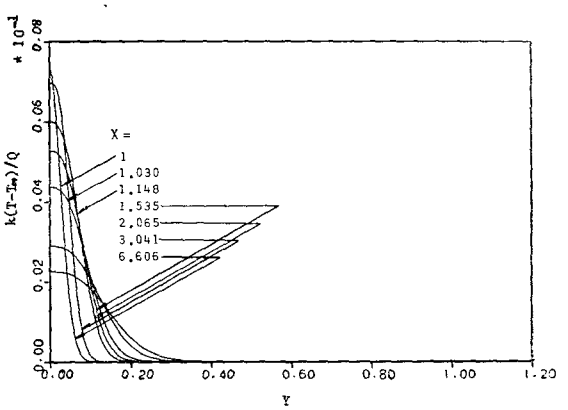

Fig. 6(b) Tempreature profiles for the wall boundary layer, $Pr=10$, $Gr=10^7$.

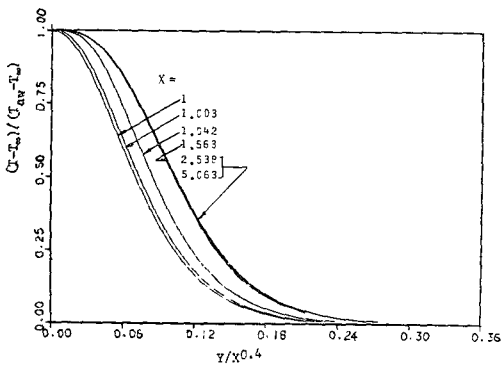

Fig. 7 Locally normalized temperature profile, Pr 1, $Gr=10^7$

profiles undergo a remarkably gradual development because of the adiabatic condition at the flat plate.

Similar to the velocity profiles, the temperature profiles again develop more slowly for the greater Prandtl numbers. It should be indicated, however, that the temperature approaches to the fully developed profile more rapidly than the velocity does, as can be seen by comparing Fig. 5 and Fig. 7. For $Pr=1$, the major development of the temperature profile is accomplished between $X=1$ and $X=1.5$ while the velocity profile is fully developed at about $X=2$.

4.2 Isothermal Flat Plate

We first inspect the heat flux from the plate. We express the heat flux from the isothermal plate as multiples of that from an identical plate which is placed in a quiescent fluid without any impinging plume. Here, we take the quantity about the latter case from the existing data[7], and will put an asterisk.

The local and global heat flux ratios are then given by

$$q/q^*=h/h^*=(x'/S)^{0.25}\left(-\frac{\partial\theta}{\partial Y}\right)_0 /\phi\theta_w^{1.25}Gr^{0.25} \qquad (11)$$

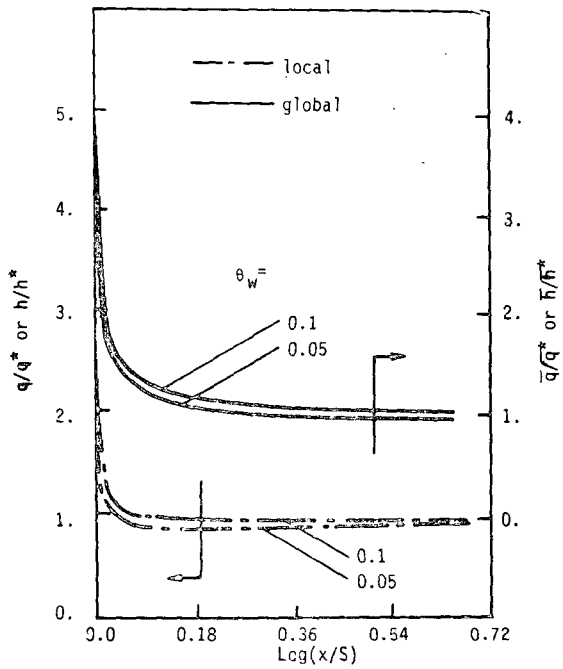

Fig. 8 Overall heat transfer coefficient and local heat flat flux along the isothemal platel

$$\bar{q}/\bar{q}^*=\bar{h}/\bar{h}^*=I/\theta_w^{0.8}(x'/S)^{0.75}(4\phi/3)Gr^{0.25} \qquad (12)$$

where

$$I=\int_0^{x'/S}\left(-\frac{\partial\theta}{\partial Y}\right)_0 d(x'/S)$$

$$\theta_w=k(T_w-T_\infty)/Q$$

$$\phi=-\theta_S'(0)/1.414$$

Here, q and $\bar{q}$ denote the local and average heat flux and h and $\bar{h}$ represent the local and average heat transfer coefficients, respectively. The results are presented in Fig. 8 for $Pr=1$ and $Gr=10^7$, in which the similarity data ϕ is taken as 0.401 from the reference (7). The global heat flux ratio in Fig. 8, presented for $\theta_w=0.1$ and 0.05, shows that the isothermal plate is very sensitive to the free plume condition in the initial developing region. The relatively large velocity of the rising plume at the instant of interception by the flat plate contributes to the initial peaks in the local and overall heat transfer near the tip. Beyond this

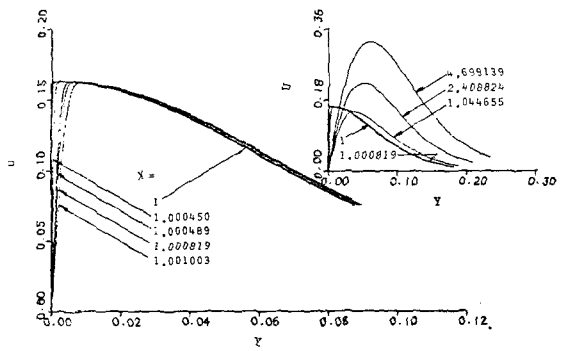

Fig. 9 Velocity profile for the isothermal pate, $Pr=1$, $Gr=10^7$, $\theta_w=0.1$

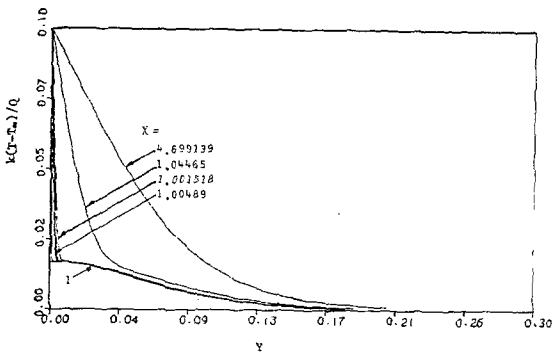

Fig. 10 Temperature profiles for the isothermal plate, $Pr=1$, $Gr=10^7$, $\theta_w=0.1$

initial developing region, both the velocity and temperature profiles asymptotically approach those of the similarity solution. There, the global heat flux ratio $\bar{q}/\bar{q}^*$ experiences gradual change and approaches the unit value ultimately. The local heat flux ratio in Fig. 8 shows similar trend to that of the global heat flux explained so far.

Here, we can conclusively speak that the finite velocity of the incident plume in general enhance the heat flux from the initial region near the leading edge of the plate. However, far downstream the isothermal plate does not feel the existence of the incident free plume any more, hence the similar profiles are attained.

In Figs. 9 and 10, the velocity and the temperature are shown as functions of Y, repectively. As the incident plume impinges against the flat plate, it is immediately influenced by the already-existing hydraulic and thermal boundary layers of the flat plate. As the buoyant flow streams upward from the leading edge of the flat plate, the plume and the inherent wall boundary layer should compromise to constitute a new overall boundary layer. This emergence of a third new boundary layer in the downstream direction is clearly seen in Figs. 9 and 10. In Fig. 10, in the near distance (x'/S) from the leading edge of the plate, the new thermal boundary layer does not penetrate very far into the old boundary layer. However, with increasing x'/S, the new thermal boundary layer grows big enough to engulf the old one. That is, the wall boundary layer effect consequently becomes dominating in the downstream direction.

5. Conclusion

We have analyzed the interaction of a wall boundary layer and a free shear layer, which is induced by a horizontal line heat source below the vertical flat plate. For the adiabatic vertical flat plate, it is found that the velocity and temperature profiles becomes fully developed downstreamwise and have the similar profiles. The development of these similar profiles is dependent on the Prandtl number. In the fully developed region, the maximum velocity increases monotonically as $X^{0.2}$, while the maximum temperature decreases as $X^{-0.6}$. The maximum velocity retardation, which is increased in its degree for higher Prandtl number, is seen in the initial stage of development due to the interaction between the skin friction and the buoyancy force.

For the isothermal vertical flat plate, the heat transfer from the plate is very sensitive

to the presence of the line heat source near the leading edge of the plate. The finite-velocity approach of the incident flow exerts a dominant influence on the heat transfer in the initial region over the negative role of the pre-heated thermal condition of the plume.

The temperature and the velocity profiles presented in the present paper substantialize the idea how the wall boundary layer on the isothermal plate grows within the already existing free shear layer. With increasing downstream distance, the new growing boundary layer engulfs the old one to form a similar profile eventually.

References

1) B. Gebhart, L. Pera and A.W. Schorr, "Steady Laminar Natural Convection Plume Above a Horizontal Line Source", Int. J. Heat and Mass Transfer, Vol. 13, pp. 161~171, 1970

(2) A.M. Schorr and B. Gebhart, "An Experimental Investigation of Natural Convection Wakes Above a Line Heat Source", Int. J. Heat and Mass Transfer, Vol. 16, pp. 557~571, 1973

(3) T. Fujii, I. Morioka and H. Uehara, "Buoyant Plume Above a Horizontal Line Heat Source", Int. J. Heat and Mass Transfer, Vol. 16, pp. 755~768, 1973

(4) S.V. Patankar and D.B. Spalding, *Heat and Mass Transfer in Boundvry Layers*, 2nd ed., Intertext Books, London, 1970

(5) E.M. Sparrow, S.V. Patankar and M. Faghri, "Natural Convection Heat Transfer From the Upper Plate of a Collinar, Separated Pair of Vertical Plates", ASME J. Heat Tansfer, Vol. 102, pp. 153~157, 1980

(6) Y. Jaluria and B. Gebhart, "Buoyancy-induced Flow Arising From a Line Heat Source on an Adiabatic Vertical Surface", Int. J. Heat and Mass Transfer, Vol. 20, pp. 153~157, 1977

(7) Y. Jaluria, *Natural Convection Heat and Mass Transfer*, lst ed., Pergamon Press, London, 1980